Characterization of $PrIr_4Sb_8Sn_4$ Using X – Ray Diffraction

Jessica M. Wile
Department of Physics
Kalamazoo College

In Collaboration with:
Dr. Clement Burns
Physics Department
Western Michigan University

Supervised by:
Dr. Tom Askew
Department of Physics
Kalamazoo College

A paper submitted in partial fulfillment of the requirements for the degree of Bachelor of Arts at Kalamazoo College
2019

Acknowledgements

First and foremost, I would like to thank Dr. Clement Burns for allowing me to assist with his research and for his invaluable guidance throughout the duration of this project. I would also like to thank his graduate assistant, Matthew Cook, for his continued guidance and support.

Next, I would like to thank the Kalamazoo College Math and Physics departments for providing me with an exceptional education and for providing me with the foundation for a life time of learning. I would also like to thank the Heyl Scholarship Fund for funding my research project.

Finally, I would like to express my profound gratitude towards my SIP Advisor, Dr. Askew, for his constant support and guidance throughout the entire SIP process and for continually pushing me towards my full potential. I most certainly could not have done this without him.

Abstract

Crystals of a previously unknown type with the composition $PrIr_4Sb_8Sn_4$ were grown using methods that are described. An initial attempt to determine the crystal structure was made using small crystals and x-ray diffraction methods. Experimental difficulties prevented us from making an initial determination of the crystal structure. Further experiments will be necessary.

Contents

1. Introduction

1.1 Structural Characteristics of a Crystal **1**

1.2 X – Ray Diffraction and $PrIr_4Sb_8Sn_4$ Crystals **2**

2. Research Methods

2.1 Crystalline Formation **5**

2.2 X – Ray Diffraction **6**

3. Results **10**

4. Conclusion **14**

5. References **15**

List of Figures

1. A cubic three – dimensional lattice. Each corner represents a lattice point and each individual cube inside the lattice represents a unit cell 1
2. Diffraction of x-rays by a crystal where A, B, and C are parallel planes of atoms with d' spacing between them 2
3. $PrIr_4Sb_8Sn_4$ single crystal on the mount as seen from the x – ray machine camera (left) and from under a microscope (right) 6
4. Set up of the SMART Apex2 x – ray diffractometer system (left) and the SMART goniometer components (right) 7
5. Depicts Kα and $K\beta$ emission lines for a copper source 7
6. Image of the initial still scan of the $PrIr_4Sb_8Sn_4$ single crystal. Limited and uniform spotting indicate the crystal quality is acceptable to analyze with XRD 8
7. Displays the cell information obtained from the single crystal as found by the x – ray diffractometer 10
8. The green bar displays the lattice I type recommended by the software which was determined by the mean intensities and the mean intensities/sigma . . . 11
9. This figure displays the structure produced by using the "Auto – structure" function of the program 12
10. Displays the statistics chart regarding the number of diffraction peaks, redundancies, mean intensities and R values 12

11. Integration graphs of the average correlation coefficient vs. image, average spot intensity vs. image, and the error vs. image 13

Characterization of $PrIr_4Sb_8Sn_4$ Using X – Ray Diffraction

Jessica M. Wile

Introduction

Structural Characteristics of a Crystal

The intensity with which an x – ray diffracts depends on the location of the atoms in the unit cell. A crystal structure is defined by its lattice along with periodic arrangement of atoms within a unit cell (Ashcroft & Mermin 1976). A lattice consists of all points with position vectors **R** of the form $\mathbf{R} = n_1\mathbf{a}_1 + n_2\mathbf{a}_2 + n_3\mathbf{a}_3$, where $\mathbf{a}_1$, $\mathbf{a}_2$, $\mathbf{a}_3$ are any three vectors not all in the same plane and n_1, n_2, and n_3 range through all integral values as shown in Figure 1. The vectors $\mathbf{a}_i$ are known as the primitive vectors and span the lattice (Ashcroft & Mermin 1976).

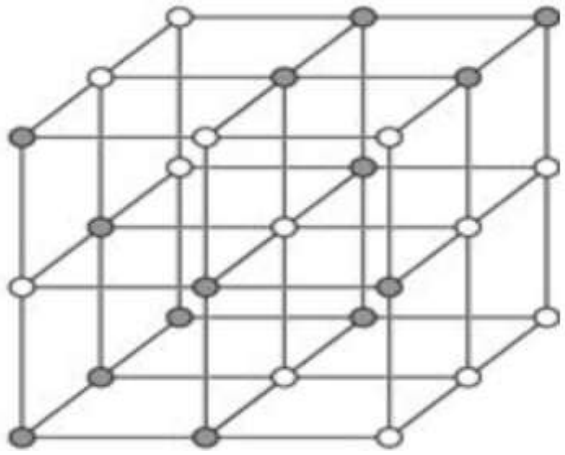

Figure 1: A cubic three – dimensional lattice. Each corner represents a lattice point and each individual cube inside the lattice represents a unit cell. Data retrieved from https://www.nature.com/articles/nphys645.

The space group denotes the vectors which define the geometry of the unit cell, specifically the cubic structure of the crystalline compound investigated in this study (Cullity & Stock 2001).

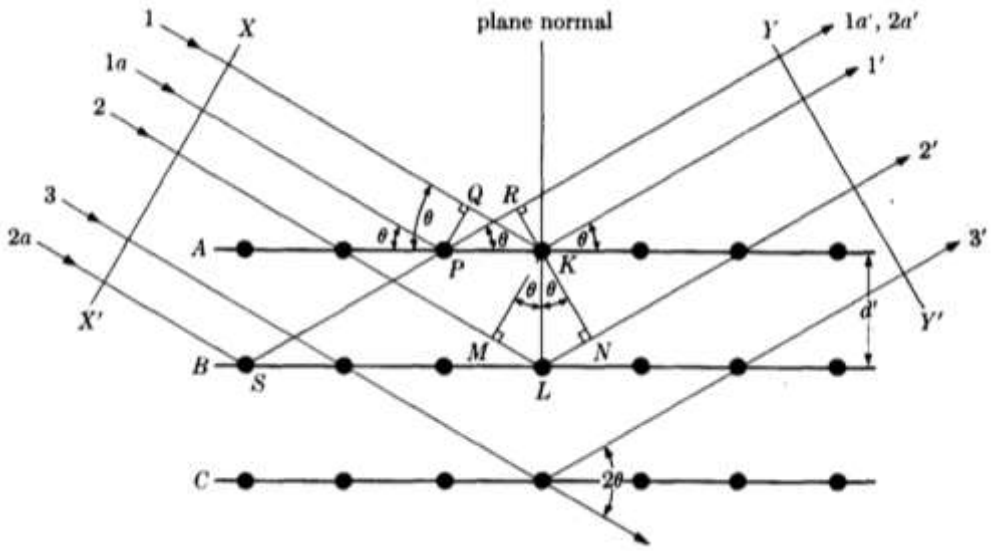

Figure 2: Diffraction of x-rays by a crystal where A, B, and C are parallel planes of atoms with d' spacing between them. Data retrieved from *Elements of X-Ray Diffraction* (3rd ed.).

X – Ray Diffraction and $PrIr_4Sb_8Sn_4$ Crystals

X – ray diffraction (XRD) is a common technique employed to characterize the crystalline structure of new compounds. In general, diffraction occurs when light is scattered by a periodic array with long-range order, producing constructive interference at specific angles (Speakman n.d).

Diffraction is a scattering phenomenon defined by the interaction between x – rays and atoms (Cullity & Stock 2001). Consider Figure 2 where *K* and *P* are atoms in the first parallel plane of a crystal. We can assume that a monochromatic x – ray beam of wavelength λ is incident on this crystal at an angle theta, θ. This angle is measured between the incident x – ray beam and a parallel plane and is known as the

Bragg angle, θ. Rays **1** and **1a** are scattered in phase only in the directions of **1'** and **1a'** as they satisfy the condition for Braggs Law, $n\lambda = 2d'sin\theta$, because their path difference is equal to a whole number, n, of wavelengths. This equation also holds for rays scattering on adjacent planes. When all of the scattered x – rays are in phase, they produce constructive interference and form a diffracted beam. This diffracted beam is much weaker than the initial incident beam because only a fraction of the x – rays that are scattered are in phase with one another (Cullity & Stock 2001).

X – ray scattering is determined by the wavelength of the x – rays along with the geometry of the unit cell (Wlodawer et al. 2007). The use of XRD in defining a crystalline structure was first discovered in 1912 when Max von Laue proposed that x – rays have a similar order of magnitude as the spacing between adjacent atoms in crystals (Beiser 1985). It is important to understand the crystalline structure as it is useful in identifying properties of that particular compound such as electrical conductivity, melting point, etc. Knowing these properties can lead to new scientific discoveries. Historically, the technique of XRD has been used to characterize the double helical structure of DNA. Using Rosalind Franklin's work with XRD on DNA, Watson and Crick were able to solve the previously unknown double helical structure of DNA (Watson & Crick 1953). Another compound in which XRD was useful in structure determination is that of the diamond (Bragg & Bragg 1913). The diamond has both cosmetic and industrial value. Without knowing its structure, it would be impossible to know how the structure relates to its use in new technologies. There would be no way of knowing how the diamond could have

further industrial value for the uses of polishing, drilling, etc. In the instances of both DNA and the diamond, the results produced by XRD were consistent with structural characteristics found by other methods. X – ray diffraction then proves to be a reliable method to begin characterizing the crystalline structure of newly synthesized compounds.

The class of compounds with which this study is concerned is skutterudites. Filled skutterudite materials are compounds that exhibit superconductivity as well as some magnetic phenomena and fermion behaviors (Luo et al. 2015). There has been recent interest in synthesizing and characterizing new filled skutterudite materials because of these unique physical properties. In the last few decades, heavy fermion and superconductivity behavior have been observed in a subset of heavy fermion compounds containing Praseodymium (Bauer et al. 2002). Crystalline filled skutterudite $PrOs_4Sb_{12}$, a close relative of $PrIr_4Sb_8Sn_4$, has been characterized by x – ray diffraction and exhibits both of these properties. $PrIr_4Sb_8Sn_4$ is partially substituted, which might change the electronic structure, but not the overall number of electrons.

In this study we attempted to synthesize $PrIr_4Sb_8Sn_4$ using high temperature and a flux method. In order to confirm that we had synthesized the compound of interest to be used for further research, we first needed to characterize its structure by x – ray diffraction which was the objective of this study.

Research Methods

Crystalline Formation

To produce the $PrIr_4Sb_8Sn_4$ crystalline compound, Praseodymium (Pr) was weighed and cut inside a glove box to prevent Praseodymium from reacting with the air. Then Iridium (Ir), Antimony (Sb), and Tin (Sn) were weighed in proper proportions of $PrIr_4Sb_{13.33}Sn_{6.66}$ for single crystal flux growth. The exact weights were as follows: Pr ~ 0.1378g, Ir ~ 0.756g, Sb ~ 1.570g, and Sn ~ 0.78g. These proportions were chosen based on previous experimental crystal growths of $PrOs_4Sb_{20}$. A quartz tube then was carbon coated with pyrolysis of acetone. Praseodymium and Iridium were loaded into an ampoule following Antimony and Tin. The ampoule was evacuated and filled with Argon to approximately 500 mbar. The process was repeated three times. Subsequently, the ampoule was sealed with a Hydrogen/Oxygen torch. The compound was then placed in a high temperature furnace. The furnace increased from room temperature to 950° Fahrenheit at 200°F/hr. For 24 hours, the furnace was maintained at a temperature of 950° Fahrenheit to allow proper mixing. The furnace was then cooled down to 650° Fahrenheit at 1°F/hr, followed by a cooling period down to room temperature at 200°F/hr. The crystals were then etched in an aqua region in order to isolate them.

The crystals were cleaved using a scalpel under a microscope in order to obtain a single, cubic crystal suitable for x – ray diffraction. Based on the 0.5 mm beam, the crystal can be at most 0.25 mm x 0.25 mm x 0.25 mm with a 0.43 mm

diagonal, where a unit cell of this size is considered to be the maximum suitable size and will produce more reflections (Bruker Corporation 2016). A cleaved single crystal was then mounted on a sample holder as shown in Figure 3.

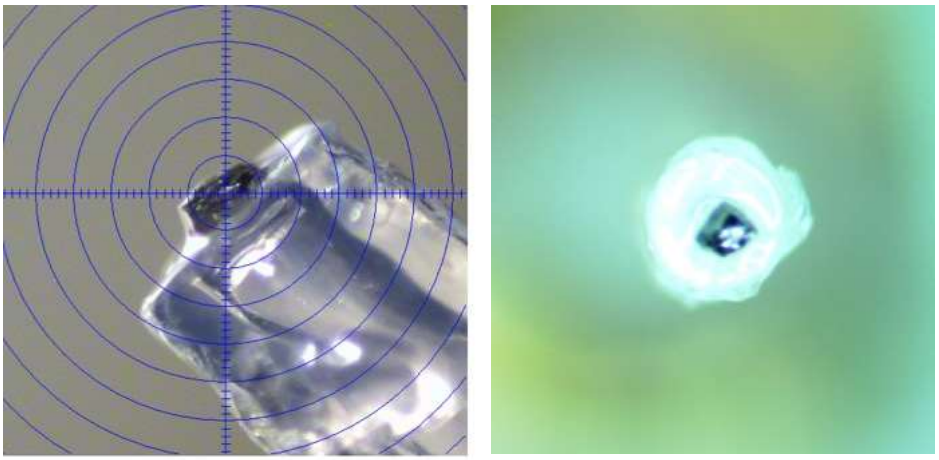

Figure 3: $PrIr_4Sb_8Sn_4$ single crystal on the mount as seen from the x – ray machine camera (left) and from under a microscope (right).

X – Ray Diffraction

X – ray diffraction data for the hypothetical $PrIr_4Sb_8Sn_4$ product was obtained using Bruker's x – ray diffractometer system contiguously with APEX3 Crystallography Software Suite. The sample was mounted and centered directly in line with an x – ray beam as shown in Figure 3 and in the setup of the x – ray system as shown in Figure 4.

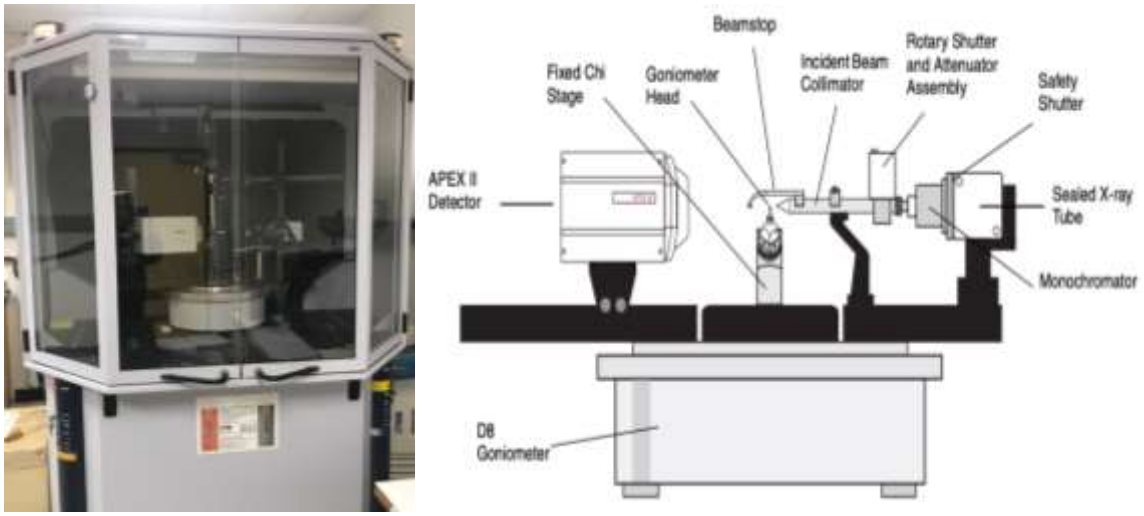

Figure 4: Set up of the SMART Apex II x – ray diffractometer system (left) and the SMART goniometer components (right). Data retrieved from http://xray.tamu.edu/pdf/manuals/apexiiusermanual.pdf.

The K780 x – ray generator is a high-frequency, solid-state x – ray generator that provides a monochromatic x – ray beam capable of operations up to 40 kV, 30 mA for Copper radiation (Bruker Corporation 2016). A beam of electrons at voltages up to 40,000 volts collides with a copper target and produces kα and kβ x – ray emission lines as shown in Figure 5 (Pak et al. 2004).

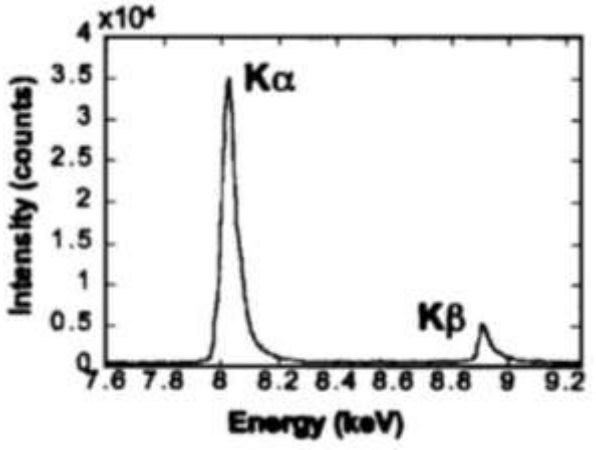

Figure 5: Depicts Kα and *K*β emission lines for a copper source (Pak et al. 2004).

A graphite crystal monochromator selects only the Kα line (λ_{avg} = 1.541838 Å for Copper radiation) emitted from the x – ray source and passes it down the collimator system from which it emerges and penetrates the crystal under study. (Bruker Corporation 2016). Since graphite is planar in structure, viewed from the edge it looks very much like Figure 2 and gives a very strong diffraction pattern making it ideal for this purpose. It is essential to have only one wavelength and energy present in the x – ray beam so that the crystal produces just one diffraction pattern that can be imaged on the camera.

The sample was repeatedly rotated, and adjustments were made to the x, y, and z positions on the goniometer in order to calibrate the beam. "Spin Phi 90°" and "Spin Phi 180°" spun the mounted sample holder around its axis by both 90° and 180° to ensure that the crystal stayed in the line of the x – ray beam. A beam stop is aligned with the beam in order to minimize scattered x – rays after the beam passes through the crystal (Bruker Corporation 2016). A still scan was collected to determine whether or not the sample was suitable for x – ray diffraction analysis as shown in Figure 6.

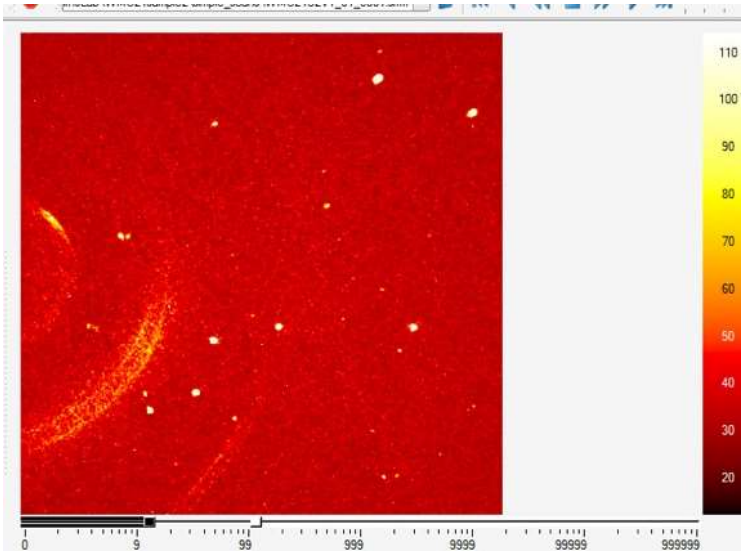

Figure 6: Image of the initial still scan of the $PrIr_4Sb_8Sn_4$ single crystal. Limited and uniform spotting indicate the crystal quality is acceptable to analyze with XRD.

The sample displayed limited spotting, indicating it was sufficiently uniform and of appropriate size to proceed with XRD. The faint rings are from the glue on the sample holder and the sample holder itself as the x – ray beam cannot penetrate amorphous solids. Once the machine was calibrated and the sample was determined to be suitable for the technique, XRD was initiated. APEX3 software collected data regarding the structure of the crystal along with the reflections and intensities from the x – ray beam during the XRD which was later used to analyze the structure of the sample.

Results

The x – ray machine defined the unit cell constants for the $PrIr_4Sb_8Sn_4$ single crystal to be 9.2666 Å x 9.2666 Å x 9.2666 Å with 90° angles between the unit cell edges depicting a cubic lattice structure as expected as shown in Figure 7.

Figure 7: Displays the cell information obtained from the single crystal as found by the x – ray diffractometer.

Figure 8 displays the predicted lattice type shown in green that best agrees with the unit cell. The lattice type is determined by the mean intensities of the reflections. Having a higher probability of a particular lattice type is represented by a wider and higher peak as represented in Figure 8.

Figure 8: The green bar displays the lattice I type recommended by the software which was determined by the various mean intensities and the mean intensities/sigma.

The auto – structure shown in Figure 9 is a result that was not expected. It is difficult to determine which atoms are connected and the ratios of the atoms to one another do not appear to be accurate. It is evident that this model is inaccurate as one of the atoms is not attached to the main structure.

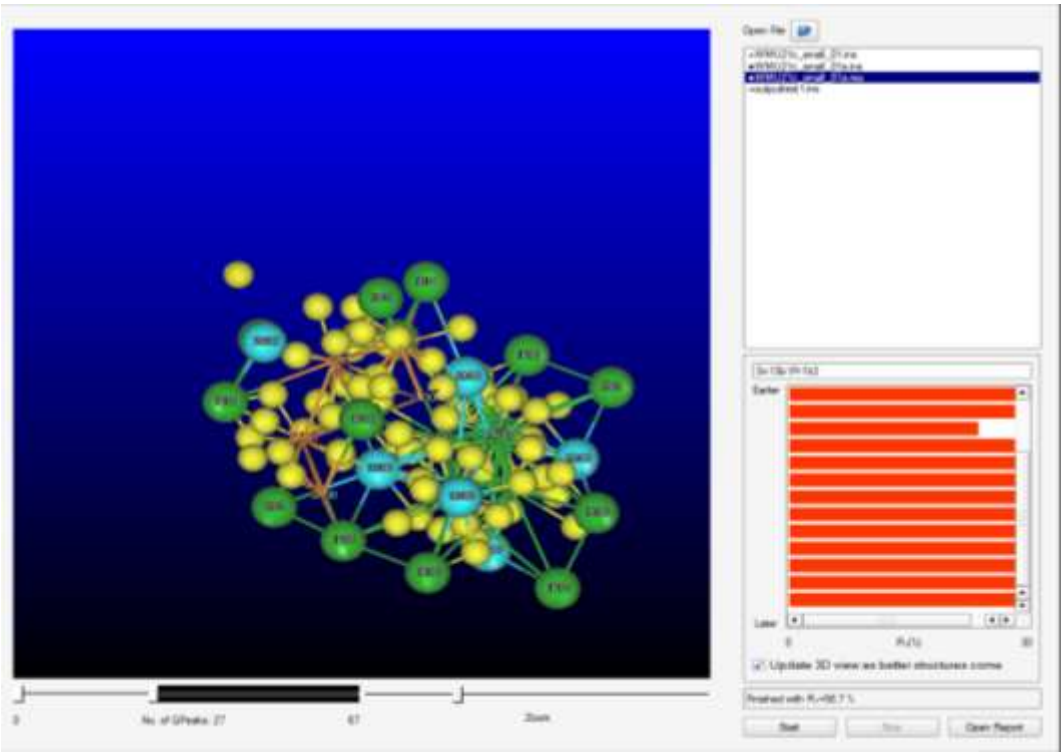

Figure 9: This figure displays the structure produced by using the auto – structure function of the program.

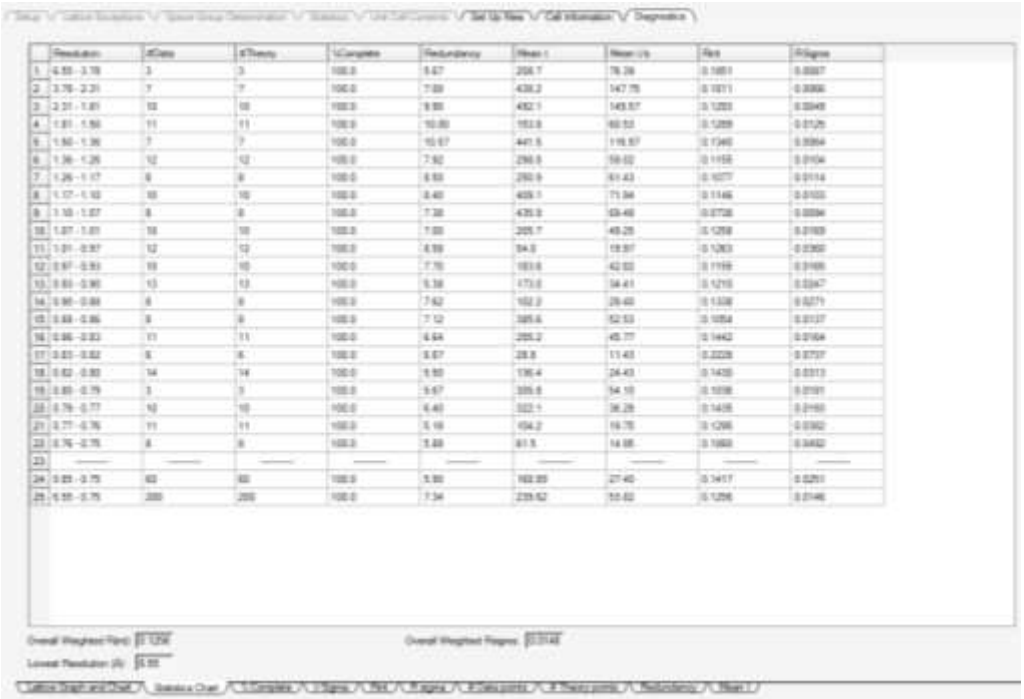

Figure 10: Displays the statistics chart regarding the number of diffraction peaks, redundancies, mean intensities, and R values.

As shown in Figure 10 above, the number of diffraction peaks matches the number of diffraction peaks in theory as confirmed by the % completeness. The redundancy measures the average number of measurements per individual, symmetrically unique reflections (Wlodawer et al. 2007). The redundancy should decrease as the resolution decreases and Figure 10 approximately follows this trend. The R – intensity defines the agreement between the results from the XRD and the parameters that were initially defined for this compound. As seen in Figure 11 below, the correlation coefficient, R – value, is rather high while the average spot intensity and error have a wider range. This may have been a result of the crystal quality or geometry of the crystal.

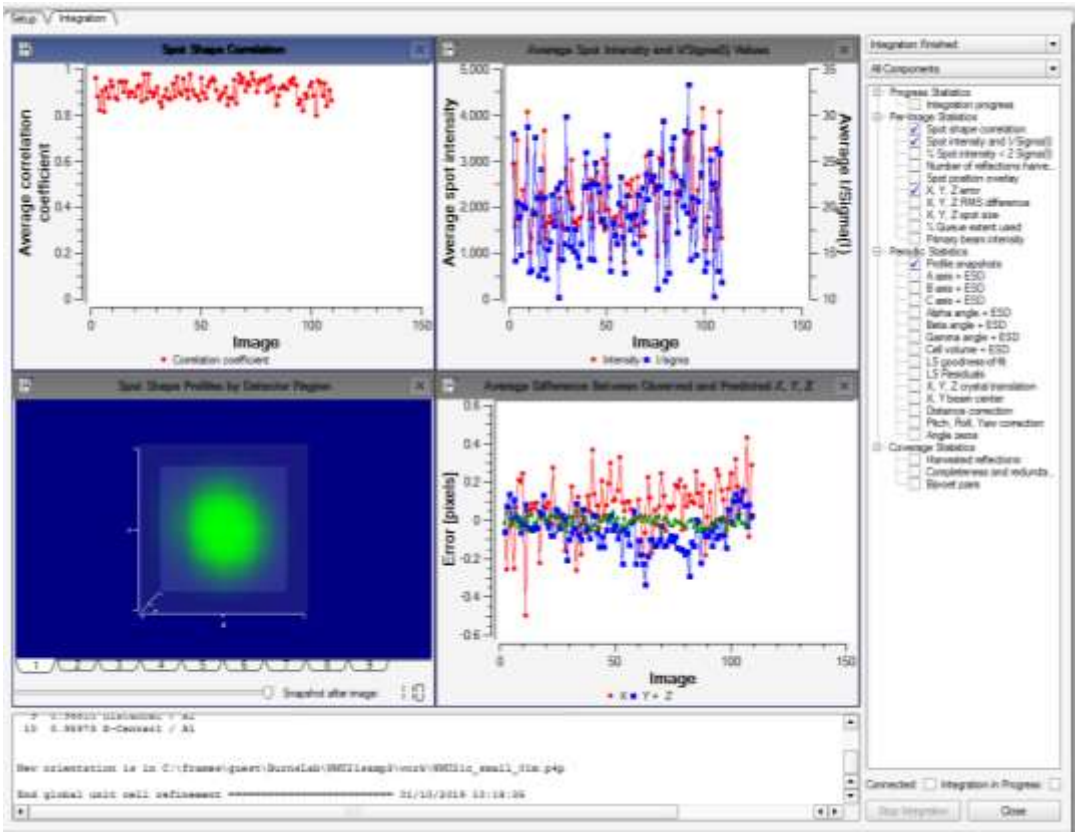

Figure 11: Integration graphs of the average correlation coefficient vs. image, average spot intensity vs. image, and the error vs. image.

Conclusion

The overall predicted structure of $PrIr_4Sb_8Sn_4$ does not appear to be an accurate representation of an actual crystal structure. This inaccuracy could have resulted from the crystal quality not being as pristine as initially thought. The crystal may not have been a single crystal despite its pristine appearance. The crystal could also have been too small so that it simply did not produce enough diffracted x – rays for proper analysis. The possibility exists that this particular compound has a very strange crystal structure which we are beginning to probe and cannot analyze using existing structures in the software library.

Further investigation should include XRD studies for multiple crystals from the same growth process to understand possible sources of error. The XRD proved to be useful in determining the symmetry and lattice constants of the crystal, but was insufficient in determining the structure of the crystal. Further progress indicates the need for repeated experiments involving different crystals so that the structure of this particular skutterudite can be determined.

References

1. Ashcroft, N. W. & Mermin, D. N. (1976). *Solid State Physics* (1st ed.). Cengage Learning.
2. Bauer, E., Frederick, N., Ho, P., Zapf, V., & Maple, M. (2002). Superconductivity and Heavy Fermion Behavior in $PrOs_4Sb_{12}$. *Physical Review B,65*(10), 1005061-1005064.
3. Beiser, A. (1985). *Perspectives of Modern Physics*. New York: McGraw-Hill.
4. Bragg, W., & Bragg, W. (1913). The Structure of the Diamond. *Proceedings of the Royal Society of London. Series A, Containing Papers of a Mathematical and Physical Character, 89*(610), 277-291. Retrieved from http://www.jstor.org.libproxy.library.wmich.edu/stable/93489
5. Bruker Corporation. (2016). *APEX3 Crystallography Suite User Manual* [Pamphlet]. Madison, WI: Bruker AXS.
6. Cullity, B. D. & Stock, S. R. (2001). *Elements of X-Ray Diffraction* (3rd ed.). NJ: Prentice Hall.
7. Kohgi, M. M., Iwasa, K., Nakajima, M., Sato, H., Aoki, Y., Sugawara, H., . . . Gukasov, A. (2003). Evidence for magnetic-field-induced quadrupolar ordering in the heavy-fermion superconductor $PrOs_4Sb_{12}$. Journal of the Physical Society of Japan, 72(5), 1002-1005.
8. Luo, H., Krizan, J. W., Muechler, L., Haldolaarachchige, N., Klimczuk, T., Xie, W., . . . Cava, R. J. (2015). A large family of filled skutterudites stabilized by electron count. *Nature Communications,6*(1). doi:10.1038/ncomms7489
9. Pak, A., Gregori, G., Knight, J., Campbell, K., Price, D., Hammel, B., . . . Glenzer, S. (2004). X-ray line measurements with high efficiency Bragg crystals. *Review of Scientific Instruments, 75*(10), 3747-3749.
10. Speakman, S. A. (n.d.). *Basics of X-Ray Powder Diffraction*. Lecture presented at MIT. Retrieved from http://prism.mit.edu/xray
11. Watson, J., & Crick, F. (1953). MOLECULAR STRUCTURE OF NUCLEIC ACIDS: A Structure for Deoxyribose Nucleic Acid. *Nature*.
12. Wlodawer, A., Minor, W., Dauter, Z., & Jaskolski, M. (2007). Protein crystallography for non-crystallographers, or how to get the best (but not more) from published macromolecular structures. *The FEBS journal*, *275*(1), 1-21.